DOI: 10.1002/ejic.200600448

Synthesis, Solid-State Structures, and EPR Spectroscopic Studies on Polycrystalline and Single-Crystal Samples of α-Diimine Cobalt(II) Complexes

Vítor Rosa,[a] Pablo J. Gonzalez,[a] Teresa Avilés,*[a] Pedro T. Gomes,[b] Richard Welter,*[c] Alberto C. Rizzi,[d] Mario C. G. Passeggi,[d,e] and Carlos D. Brondino*[d]

Keywords: Cobalt(II) complexes / α-Diimine ligands / Single-crystal X-ray diffraction / EPR spectroscopy

Cobalt compounds of the general formula [CoX_2(α-diimine)], where X = Cl or I and the α-diimines are 1,4-diaryl-2,3-dimethyl-1,4-diaza-1,3-butadiene (Ar-DAB) and bis(aryl)-acenaphthenequinonediimine (Ar-BIAN) were synthesized by the direct reaction of the anhydrous cobalt salts $CoCl_2$ or CoI_2 and the corresponding α-diimine ligand in dried CH_2Cl_2. The synthesized compounds are [Co(Ph-DAB)Cl_2] (**1a**), [Co(*o*,*o*′,*p*-$Me_3C_6H_2$-DAB)Cl_2] (**1b**), and [Co(*o*,*o*′-$iPr_2C_6H_3$-DAB)Cl_2] (**1c**) with the ligands Ar-DAB, and also [Co(*o*,*o*′,*p*-$Me_3C_6H_2$-BIAN)I_2] (**2′b**) with the ligand Ar-BIAN. The crystal structures of all the compounds were solved by single-crystal X-ray diffraction. In all cases the cobalt atom is in a distorted tetrahedron, which is built up of two halide atoms and two nitrogen atoms of the α-diimine ligand. X-band EPR measurements of polycrystalline samples performed on compounds **1b**, **1c**, and **2′b** indicate a high-spin Co^{II} ion (S = 3/2) in an axially distorted environment. Single-crystal EPR experiments on compounds **1b** and **1c** allowed us to evaluate the orientation of the ***g*** tensor in the molecular frame.

Introduction

Cobalt is a 3d transition metal element that has been extensively studied over the last decades. Interest in cobalt compounds arises from their participation in many different processes, from industrial and technological applications as catalysts to the essential role in several biological systems of central importance in nature.[1–5]

A large number of late transition metal complexes bearing α-diimine[6] ligands have been extensively studied in the commercial production of polyolefin from ethene and propene.[7,8] However, reports on cobalt complexes containing this type of ligands are still scarce.[9] Recently, some results from the insertion polymerization of ethylene have been reported using tetrahedral Co^{II} complexes with related ligands.[10] α-Diimine ligands have also been the subject of different studies regarding the relative binding strengths,[11] as well as their reactivity with main group metals.[12]

[a] REQUIMTE/CQFB, Departamento de Química, FCT, Universidade Nova de Lisboa,
Caparica 2829-516, Portugal
E-mail: tap@dq.fct.unl.pt
[b] Centro de Química Estrutural, Instituto Superior Técnico, Av. Rovisco Pais, 1049-001 Lisboa, Portugal
[c] Laboratoire DECOMET, ILB Université Louis Pasteur 4, rue Blaise Pascal, 67000 Strasbourg, France
E-mail: welter@chimie.u-strasbg.fr
[d] Departamento de Física, Facultad de Bioquímica y Ciencias Biológicas, Universidad Nacional del Litoral, C.C. 242, 3000 Santa Fe, Argentina
E-mail: brondino@fbcb.unl.edu.ar
[e] INTEC, Universidad Nacional del Litoral, Güemes 3450, 3000 Santa Fe, Argentina

Less information exists about the magnetic properties of these types of compounds. The Co^{II} ions can be present in two different spin configurations (high, S = 3/2 or low, S = 1/2), but in general they adopt the high-spin configuration when they are in distorted coordination environments. A large amount of work has focused on the study of the magnetic properties of Co^{II} compounds in different coordination environments, some of them analyzing Co^{II} in metalloproteins and compounds of biological interest.[13–19] Most of them have involved EPR spectroscopic studies on powder or frozen solutions and the evaluation of thermodynamic properties such as magnetic susceptibility and magnetization. In contrast, only a small amount of work related to high-spin Co^{II} compounds having a low symmetry has been devoted to the study of the correlation between the principal values and directions of the ***g*** tensor.[20–24] This type of information, which can be only obtained from oriented single-crystal EPR spectroscopic experiments, is essential to understand the electronic and magnetic properties of the systems containing Co^{II} ion complexes.

We report herein the synthesis and characterization of a series of Co^{II} complexes of general formula [CoX_2(α-diimine)], where X = Cl or I and the α-diimines are 1,4-diaryl-2,3-dimethyl-1,4-diaza-1,3-butadiene (Ar-DAB) or bis(aryl)acenaphthenequinonediimine (Ar-BIAN), namely, [Co(Ph-DAB)Cl_2] (**1a**), [Co(*o*,*o*′,*p*-$Me_3C_6H_2$-DAB)Cl_2] (**1b**), [Co(*o*,*o*′-*i*$Pr_2C_6H_3$-DAB)Cl_2] (**1c**), and [Co(*o*,*o*′,*p*-$Me_3C_6H_2$-BIAN)I_2] (**2′b**). Their crystal structures were solved by single-crystal X-ray diffraction. Powder samples

of compounds **1b**, **1c**, and **2′b** were studied by EPR spectroscopy. Compounds **1b** and **1c** were also studied by single-crystal EPR spectroscopy. The EPR spectroscopic results obtained from both powder and single-crystal samples were correlated with the structures of the compounds.

Results and Discussion

General Characterization of the Compounds

The reaction of equimolar quantities of CoX_2, where X = Cl or I, and α-diimine ligands in dried CH_2Cl_2 at room temperature yields crystalline solids of compounds of the general formula [Co(α-diimine)X_2] in c.a. 75 to 85% yield (Scheme 1).

Elemental analyses, mass spectrometry, IR, X-ray, and EPR spectroscopy were used to characterize all of the synthesized compounds. The analytical data of the synthesized compounds are shown in Table 1.

The IR spectra of the cobalt complexes recorded as Nujol mulls display medium absorption bands in the region $\tilde{\nu}$ = 1643–1621 cm^{-1}, this is the absorption region for ν(C=N). Bands assigned to C=N stretching vibrations of the free ligand were observed in the region $\tilde{\nu}$ = 1674–1633 cm^{-1}. The bands in the complexes are shifted to lower wavenumbers, which is a criterion for the coordination of both diimine nitrogen atoms of the α-diimine ligands to the cobalt(II) ion. Selected IR absorption bands are displayed in Table 2.

Table 2. Selected IR data in Nujol mulls (values of $\tilde{\nu}$ given in cm^{-1}).

	Ar-DAB[a]	**1**	Ar-BIAN[a]	**2′**
a	1633	1643		
b	1637	1635	1674, 1650	1621
c	1639	1641		

[a] Free ligands.

Crystal Structure Descriptions

Complex 1a

The complex **1a** crystallizes in an orthorhombic space group $P2_12_12_1$. An ATOMS[25] view of the asymmetric unit of the crystal structure is shown in Figure 1. The cobalt atom is in a deformed tetrahedron, which is built up of two chloride atoms and two nitrogen atoms of the ligand [Co–Cl1: 2.214(1) Å; Co–Cl2: 2.210(1) Å; Co–N1: 2.043(4) Å;

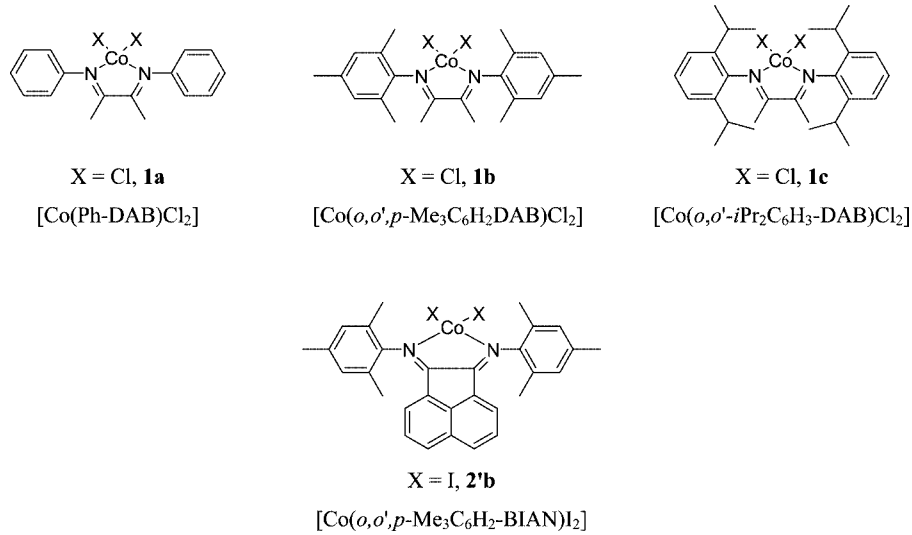

Scheme 1. Synthesized complexes.

Table 1. Analytical data.

	Molecular mass [g mol^{-1}]; Molecular formula	MS(FAB) m/z[a]	Microanalysis (calcd.) [%] C	H	N	Color
1a	366.15; $C_{16}H_{16}CoCl_2N_2$	$[L_1 + H^+]$ 237 (77%); $[L_1CoL_1]^{2+}$ 265.5 (100%); $[CoL_1Cl]^+$ 330 (36%); $[L_1CoL_1Cl]^+$ 566 (71%)	52.09 (52.48)	4.34 (4.40)	7.63 (7.65)	green
1b	450.31; $C_{22}H_{28}CoCl_2N_2$	$[L_2CoCl]^+$ 414.2 (97%)	58.46 (58.68)	6.42 (6.27)	6.34 (6.22)	green
1c	576.94; $C_{28}H_{40}CoCl_2N_2 \cdot 1/2CH_2Cl_2$	$[CoL_3Cl]^+$ 498.3 (96%)	60.63 (59.33)	7.30 (7.16)	5.16 (4.86)	green
2′b	729.30; $C_{30}H_{28}CoI_2N_2$	$[L_4 + H^+]$ 417.3 (16%); $[L_4Co\ I]^+$ 602.1 (30%)	49.26 (49.41)	4.16 (3.87)	3.65 (3.84)	brown

[a] Ligand 1,4-diaryl-2,3-dimethyl-1,4-diaza-1,3-butadiene (Ar-DAB); L_1: Ar = Ph; L_2: Ar = *o*,*o*′,*p*-$Me_3C_6H_2$; L_3: Ar = *o*,*o*′-*i*$Pr_2C_6H_3$; Ligand bis(aryl)acenaphthenequinonediimine (Ar-BIAN); L_4: Ar = *o*,*o*′,*p*-$Me_3C_6H_2N$.

Co–N2: 2.034(4) Å; Cl1–Co–Cl2: 119(1)°; N1–Co–N2: 80(1)°]. The [Co–N1–C1–C3–N2] plane is strictly planar [maximum deviation from least-squares plane is 0.007(5) Å] and makes an angle of 56(1)° with both phenyl groups ([C5–C10] and [C11–C16]). No hydrogen bonds have been found in this crystal structure.

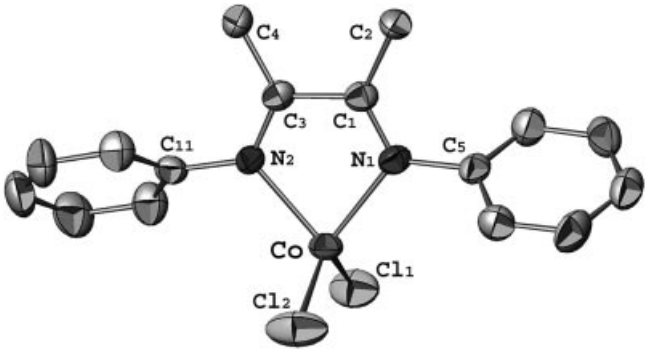

Figure 1. Molecular structure of complex **1a** (ATOMS view) with partial labeling scheme. The hydrogen atoms are omitted for clarity. The thermal ellipsoids enclose 50% of the electronic density.

Complex 1b

The complex **1b** crystallizes in a monoclinic space group $P2_1/c$. An ATOMS view of the asymmetric unit of the crystal structure is shown in Figure 2. In this case again, the cobalt atom is in a deformed tetrahedron [Co–Cl1: 2.224(1) Å; Co–Cl2: 2.212(1) Å; Co–N1: 2.050(3) Å; Co–N2: 2.051(3) Å; Cl1–Co–Cl2: 113(1)°; N1–Co–N2: 80(1)°]. Two nonclassical intermolecular hydrogen bonds have been detected (PLATON software[26]) between C3 and Cl2 [H3B–CL2: 2.75(1) Å; C3–Cl2: 3.68(1) Å; C3–H3B–Cl2: 160(1)°] and C3 and Cl1 [H3C–CL1: 2.81(1) Å; C3–Cl1: 3.78(1) Å; C3–H3C–Cl1: 169(1)°]. The angle between both phenyl groups is 14(1)° and these groups are perpendicular to the central plane [Co–N1–C1–C2–N2] [maximum deviation from least-squares plane is 0.035(2) Å] with angles of 88(1)° and 90(1)°, respectively.

Complex 1c

The complex **1c** crystallizes in an orthorhombic space group *Pnma*. An ATOMS view of the asymmetric unit of the crystal structure is shown in Figure 3. The deformed tetrahedral site around the Co atom is characterized by the following distances and angles: Co–Cl1: 2.197(2) Å; Co–Cl2: 2.201(1) Å; Co–N: 2.050(3) Å Cl1–Co–Cl2: 113(1)°; N1–Co–N2: 80(1)°. Compared to that observed in both the previous structures, the plane containing the Co atom is not well fitted by the least-squares planes calculation (SHELXL-97)[27] with a maximum deviation from the plane of 0.112(3) Å for both nitrogen atoms. This pseudo plane makes an angle of 87(1)° with both phenyl groups (identical by symmetry), the latter are tilted with an angle of 15(1)°, one compared to the other. At least two nonclassical intramolecular hydrogen bonds have been detected (PLATON software) between C9 and N [H9–N: 2.43(1) Å; C9–N: 2.94(1) Å; C9–H9–N: 111(1)°] and C12 and N [H12–N: 2.38(1) Å; C12–N: 2.88(1) Å; C12–H12–N: 110(1)°].

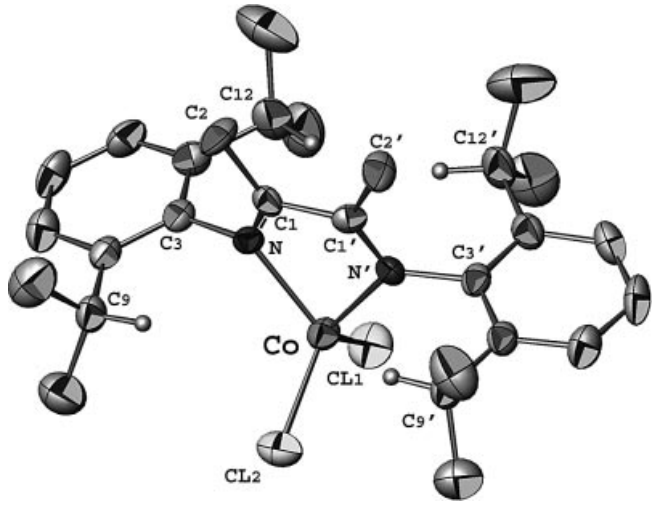

Figure 3. Molecular structure of complex **1c** (ATOMS view) with partial labeling scheme. The hydrogen atoms are omitted for clarity. The thermal ellipsoids enclose 50% of the electronic density. Operators for generating equivalent atoms: $x, y, -z+3/2$.

Complex 2′b

The complex **2′b** crystallizes in an orthorhombic space group *Pcca*. An ATOMS view of the asymmetric unit of the crystal structure is shown in Figure 4. The deformed tetrahedral site around the Co atom is characterized by the

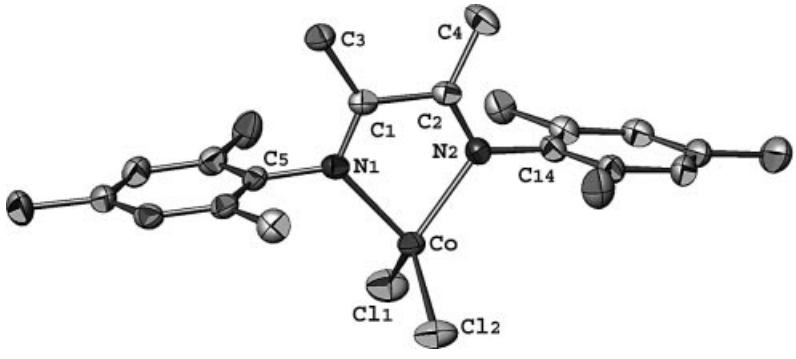

Figure 2. Molecular structure of complex **1b** (ATOMS view) with partial labeling scheme. The hydrogen atoms and the solvent molecules (CH_2Cl_2) are omitted for clarity. The thermal ellipsoids enclose 50% of the electronic density.

following distances and angles: Co–I: 2.509(1) Å; Co–N: 2.05(1) Å; I–Co–I′: 111(1)°; N–Co–N′: 82(1)°. The angle between both phenyl groups is 14(1)° and these groups make an angle of 85(1)° with the central plane [Co–N–C1–C1′-N′] [maximum deviation from least-squares plane is 0.001(4) Å]. It is important to note that the molecule of complex **2′b** is placed on a crystallographic mirror i.e. the following atoms are on the mirror (see Figure 4): Co, N, C8, C1, C2, C4, C5, C6, C7 and the corresponding equivalent atoms by the following symmetry operator: $-x$, y, $-z + 1/2$. No H bond has been detected in the case of this crystal structure. No H bond has been detected in the case of this molecular structure.

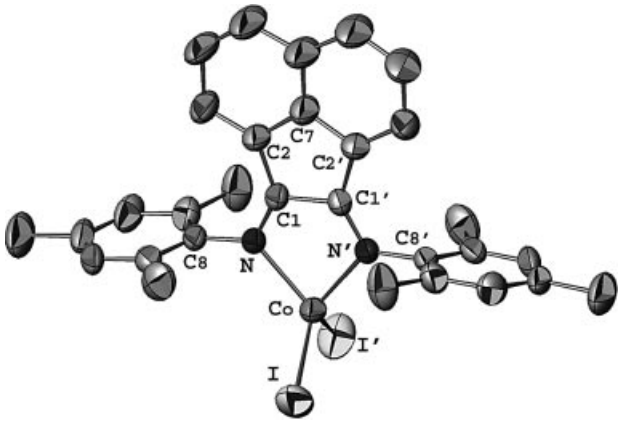

Figure 4. Molecular structure of complex **2′b** (ATOMS view) with partial labeling scheme. The hydrogen atoms and the solvent molecules (CH_2Cl_2) are omitted for clarity. The thermal ellipsoids enclose 50% of the electronic density. Operators for generating equivalent atoms: $-x$, y, $-z+1/2$.

EPR Measurements

The X-band EPR spectra of polycrystalline samples of compounds **1b**, **1c**, and **2′b** and their simulations are shown in Figure 5. The peaks broaden at higher T and disappear at ca. 50 K. The hyperfine structure expected for the 100% abundant ^{59}Co isotope ($^{59}I = 7/2$) is not observed in any of the spectra of the powder samples. The values of the g factors g_1, g_2, and g_3 are given in Table 3 and are typical for Co^{II} ions with a high spin $S = 3/2$ configuration.[17] The EPR spectrum obtained for compound **1a** (data not shown) is also compatible with a Co^{II} ion in a high-spin configuration, however, a broad signal detected in the range 500–8000 Gauss and overlapping the Co^{II} ion transitions precluded the interpretation.

In a purely tetrahedral environment, Co^{II} has the orbital singlet A_2 at lowest energy,[13,14] and since $S = 3/2$, there is a fourfold spin degeneracy. As for compounds **1b**, **1c**, and **2′b** the sites are distorted, the fourfold spin degeneracy is lifted into two Kramers doublets. If the distortion is high enough ($>>kT$) to neatly separate both doublets and the experiments are performed at low temperatures, then the observed spectra can be assigned to transitions between the states of the lowest $S' = 1/2$ spin doublet, which is expected

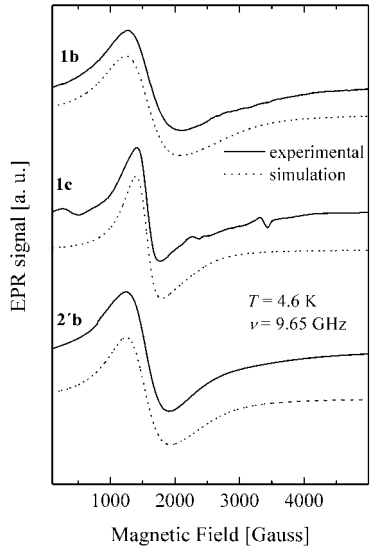

Figure 5. EPR spectra of powdered samples of compounds **1b**, **1c**, and **2′b** together with **s**imulations. The EPR parameters obtained from simulation are given in Table 3. For compound **1c**, the peak at ≈3300 Gauss corresponds to Cu^{II} impurities whereas the peak at ≈500 Gauss corresponds to a cavity background.

Table 3. EPR parameters obtained from powder and single-crystal samples for **1b**, **1c**, and **2′b**. Linewidths (ΔB) are in Gauss. The components of the crystal $\boldsymbol{g}$ tensors are expressed in the abc^* ($c^* = a \times b$) and abc coordinates system for compounds **1b** and **1c**, respectively. They were obtained by least-squares analyses of the single-crystal data.

Compound	**1b**	**1c**	**2′b**
Powder sample			
g_1	4.83(5)	4.85(5)	4.87(5)
g_2	4.37(5)	4.35(5)	4.71(5)
g_3	2.58(9)	3.12(9)	3.08(9)
ΔB_1	580(20)	280(20)	580(20)
ΔB_2	680(20)	280(20)	480(20)
ΔB_3	900(20)	600(20)	800(20)
Single crystal			
g_{aa}	2.66(2)	4.47(1)	–
g_{bb}	4.83(1)	3.12(2)	–
g_{cc}	4.32(1)	4.71(1)	–
g_{ac}	1.51(4)	0	–
g_{ab}	0	0	–
g_{cb}	0	0	–
$g_{\parallel}$	2.58(2)	3.12(2)	3.08(9)
$g_{\perp}$	2.30(1)	2.30(1)	2.40(5)
E/D	0.03	0.04	0.01

to be substantially populated.[28] The high anisotropy observed is also expected for Co^{II} compounds with a distorted tetrahedral coordination.[29,30] Since the structural data do not show relevant chemical paths connecting the metal sites that could efficiently transmit exchange interactions, the principal g values obtained from the powder spectra (Table 3) can be considered as corresponding to isolated Co^{II} ions, in which the resonance lines may be broadened by dipolar interactions. The crystal lattice of all compounds consists of a 3D network of cobalt(II) ions, with closest

metal center distances in the range 6.4–8.4 Å. This could be the cause of the unobserved hyperfine structure in the EPR powder spectra.

Single-crystal EPR spectroscopic measurements were only performed on compounds **1b** and **1c** as the size of the crystals of compounds **1a** and **2′b** was not appropriate for the EPR spectroscopic experiments. In order to understand the single-crystal EPR spectroscopic experiment, it is important to first analyze the orientation of the Co sites as well as the symmetry operations relating them within the unit cell. The unit cell of compound **1b** contains four identical Co molecules, which are related by the symmetry operations of the space group $P2_1/c$ (Figure 6a). Co1 at the general position (x,y,z) is related to Co2 by a C_{2b} rotation, as well as Co3 to Co4. Co1 and Co2 are related to Co3 and Co4, respectively, by an inversion. From the magnetic point of view, this compound can be assumed as having two magnetically nonequivalent molecules per unit cell, because the Co sites related by an inversion are indistinguishable for EPR spectroscopy.

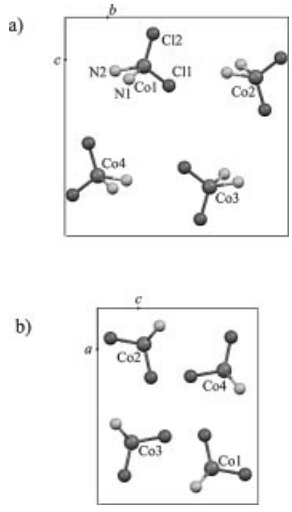

Figure 6. (a) Projection along a of the four Co^{II} ions and their ligands in the unit cell for compound **1b**. (b) Projection along b of the four Co^{II} ions and their ligands in the unit cell for compound **1c**.

Compound **1c** also has four identical Co molecules in the unit cell, related by the symmetry operations of the space group *Pnma* (Figure 6b). Co1 at the special position (x,1/4,z) is related to Co2, Co3, and Co4 by C_{2b}, C_{2a}, and C_{2c} rotations, respectively. These operations determine that there are two Co^{II} ion pairs magnetically equivalent per crystal plane, and also that the four Co sites are magnetically equivalent along the crystal a,b,c axes. The Co molecule has a mirror plane defined by the Co^{II} ion and the two Cl ligands, which is parallel to the *ca* plane. This particular local symmetry together with the space orientation of the Co molecules in the unit cell determines that the nonequivalent pairs of Co^{II} ions are equivalent in the planes *ab* and *cb*.

Single-crystal EPR spectra were recorded with the magnetic field in three orthogonal crystal planes as explained in the experimental section. In all the planes and for the two compounds we observed one resonance line for all magnetic field orientations, except around the b axis in the orthorhombic compound **1c**. In the planes *ab* and *cb* the signals become very broad around 90°, presumably because of a nonresolved hyperfine structure and therefore the position of the resonances in this zone could not be precisely evaluated. The position of the resonance line was obtained by least-squares fitting to a single Lorentzian line shape. Figure 7 shows the angular variation of the g factor as a function of the magnetic field orientation for both compounds. The data in Figure 7 were least-squares fitted to a second rank tensor $g^2(\theta,\varphi) = \boldsymbol{h.g.g.h}$, in which $\boldsymbol{h} = \sin\theta\cos\varphi$, $\sin\theta\sin\varphi$, $\cos\theta$, is the magnetic field orientation, and $\boldsymbol{g}$ is the crystal $\boldsymbol{g}$ tensor defined as the average of the molecular $\boldsymbol{g}$ tensors of the nonequivalent Co^{II} ions in the crystal lattice. The results are given in Table 3 and were used to obtain the solid lines in Figure 7. The overall symmetry of the evaluated $\boldsymbol{g}$ tensors follows the symmetry determined by the space group of each compound.

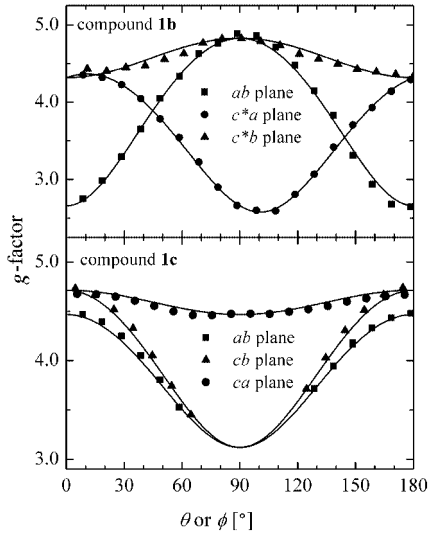

Figure 7. Angular variation of the g factor obtained from oriented single-crystal EPR spectroscopic measurements of compounds **1b** and **1c** at 9.65 GHz and T = 4.6 K. The solid lines in both plots were calculated with the components of the $\boldsymbol{g}^2$ tensor given in Table 3.

As discussed above, the angular variation of the g factor in the orthorhombic compound **1c** can be associated with a single Co^{II} ion in the planes *ab* and *cb*. By contrast, in the *ca* plane we would expect two resonance lines corresponding to the pairs Co1–Co2 and Co3–Co4. However, only one signal with a nearly isotropic angular variation was registered in this plane, which corresponds to the mirror Cl–Co–Cl plane. This fact can be due to either collapse by exchange interactions or resonance lines with similar g factors. Taking into account that from the structural data we can discard the first possibility, the observed behavior can only be explained assuming two resonance lines with similar g factors, which cannot be resolved by the EPR spectroscopic experiment at the X-band.

The orientation of the molecular ***g*** tensor for compound **1c** in the molecular frame can be evaluated from both the analysis of the geometry of coordination of the metal site and the EPR spectroscopic results. One eigenvector must correspond to the *b* crystal axis (0, 1, 0) because, as explained above, the planes *ab* and *cb* are associated with a single Co^{II} ion and the angular variation of the *g* factor is symmetric around the *b* crystal axis (g_3 = 3.12). Thus, the two remaining eigenvectors must be in the Cl–Co–Cl plane. The Co molecule can be considered as having a local pseudo-C_2 symmetry axis (–0.760, 0, 0.650) determined by the intersection of the Cl–Co–Cl plane (parallel to the *ca* crystal plane) and the N–Co–N plane. This C_2 symmetry axis must correspond to another eigenvector. The direction of the third eigenvector is straightforward (0.650, 0, 0.760). The orientation of the ***g*** tensor is shown in Figure 8. This experiment allowed us to identify the eigenvalue along the *b* crystal axis, but not the remaining two eigenvalues because the single EPR line observed in the *ca* plane corresponds to two overlapping resonance lines associated with the pairs Co1–Co2 or Co3–Co4. However, they should correspond to the highest *g* values (4.35–4.85) of the ***g*** tensor obtained from the EPR powder spectra. Because of the above discussed nonequivalence of the cobalt ions in the *ca* plane both eigenvalues can be assigned to any of the g_1 and g_2 eigenvectors. The ***g***-tensor orientation of compound **1c** is similar to that determined in the pseudo-tetrahedral dichlorobis(triphenylphosphaneoxide)cobalt(II) compound.[21] This compound shows rhombic EPR spectra (g_1 = 5.67, g_2 = 3.69, g_3 = 2.16) with the two lowest *g* values approximately included in the Cl–Co–Cl plane. Compound **1c** presents a nearly axial signal, with the lowest *g* value (g_3) lying along the normal to the Cl–Co–Cl plane. The main structural difference between both compounds is that **1c** contains the stronger N ligands instead of O ligands. On the other hand, EPR spectroscopic studies performed on a square-pyramidal Co^{II} complex showed that small deviations of the ideal C_4 site symmetry lead to important changes in the EPR spectroscopic properties of high-spin Co^{II} ions.[22] Clearly, additional experimental work on a larger number of high spin Co^{II} compounds with different structural characteristics is necessary to clarify how the different EPR spectroscopic properties can be correlated with differences in the coordination environment of the metal ion.

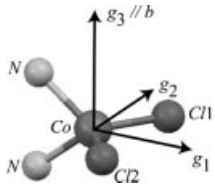

Figure 8. Orientation of the principal axes of the ***g*** tensor for the Co^{II} site in compound **1c**. The direction cosines referring to the crystal axes are: (–0.760, 0, 0.650), (0.650, 0, 0.760), and (0, 1, 0) for g_1, g_2, and g_3 = 3.12, respectively. g_1 and g_2 can take either the values 4.35 and 4.85, respectively, or vice versa.

Structural data for compound **1b** show Co sites with coordination environments and space orientations similar to that of **1c**, but the local symmetry is lower (the local mirror plane cannot be defined in this case) and the Cl–Co–Cl plane is twisted by nearly 10° from the *cb* crystal plane (Figure 6a and b). The structural similarities are reflected in Figure 7: a nearly isotropic *g* factor was obtained in the plane *c***b*, and the lowest *g* value corresponds to a direction close to the normal of the Cl–Co–Cl plane. However, having nonresolved lines in the *ab* and *cb* planes precludes determining the ***g*** tensor associated with single Co^{II} ions. Despite its lower symmetry, the coordination around Co^{II} ions in both compounds shows no significant differences and we expect a ***g*** tensor orientation similar to that shown in Figure 8 for **1b**. Although we were not able to perform single-crystal EPR experiments on compounds **2′b**, the EPR spectroscopic data from powdered samples are similar for the three compounds. Consequently, we also expect similar ***g*** tensor orientation for the compounds in which I substitutes for Cl, but single-crystal experiments are necessary to confirm this hypothesis.

After this phenomenological assignment has been made, one wonders whether it might be possible to relate the highly anisotropic *g* factors corresponding to the effective S' = 1/2 of the lowest Kramers doublet with the distortions affecting the overall state of S = 3/2. The appropriate spin Hamiltonian within the S = 3/2 can be written as [Equation (1)]

$$H = \mu_B \mathbf{BgS} + D\left(S_z^2 - \frac{1}{3}S(S+1)\right) + E\left(S_x^2 - S_y^2\right) \quad (1)$$

where D and E are the axial and rhombic zero-field splitting parameters, respectively. The quantization axis *z* is assumed to be along the axial distortion. In principle, it is not required to assume that ***g*** will have its principal axes along any of these directions.

An effective Hamiltonian within the lowest S' = 1/2 (corresponding to either the originals |3/2, ±3/2> or the |3/2, ±1/2> states) Kramers doublet can be obtained under the form[31–34]

$H_{eff} = \mu_B \mathbf{B g' S'}$

If the ground state is that derived from to the original |3/2, ±1/2> doublet and if one assumes now that the principal axes of ***g*** coincide with that of the axial distortion such that $g_z = g_\parallel$ and $g_x = g_y = g_\perp$, one gets $g'_z = g_\parallel$ while $g'_x = 2g_\perp(1 - \frac{3}{2}\frac{E}{D})$ and $g'_y = 2g_\perp(1 + \frac{3}{2}\frac{E}{D})$. Note that g'_x, g'_y, and g'_z correspond to g_2, g_1, and g_3, respectively, given in Table 3. The experimental data are not consistent with assigning the ground state to that derived from the original |3/2, ±3/2> doublet, in which $g'_z = 3g_\parallel$ while $g'_x \approx 0$ and $g'_y \approx 0$, which indicates a positive sign for the zero-field splitting parameter D. EPR data obtained from Cs_3CoCl_5 and Cs_3CoBr_5 complexes have been analyzed assuming a negative value for the D parameter,[35] and EPR spectroscopic results obtained from bis[dihydrobis(1-pyrazolyl)-

borato]Co^{II} have been interpreted assuming transitions |3/2, ±3/2>.[36] In contrast, our EPR spectroscopic data indicate a |3/2, ±1/2> ground state, in line with both theoretical and experimental results obtained from other pseudotetrahedral Co^{II} compounds.[20,21]

According to the previous discussion, adopting a coordinate system in which the z axis lies along the g_3 direction (in compound **1c** this coincides with the crystal b axis), leads to $g'_z = g_{\|}$. One can also estimate $g_\perp$ by using the other two eigenvalues obtained from the powder spectra, e.g. $g_\perp \cong (g'_x + g'_y)/4$. On the other hand, under the same assumptions, one gets

$$\left|\frac{E}{D}\right| = \frac{2\left|g'_x - g'_y\right|}{3\left(g'_x + g'_y\right)}$$

Table 3 shows these parameters obtained for the three compounds using this model. The results indicate a weak rhombic distortion for all the compounds.

Conclusions

A series of cobalt(II) complexes of general formula [Co(α-diimine)X_2], **1a**, **1b**, **1c**, and **2′b**, have been synthesized by the direct reaction of equimolar quantities of the corresponding cobalt dihalide and the α-diimine ligand in dried CH_2Cl_2 in c.a. 75 to 85% yield. Single-crystal X-ray structural data for all compounds show in all cases that the cobalt atom is in a distorted tetrahedral coordination, which is built by two halide atoms and two nitrogen atoms of the α-diimine ligand. X-band EPR measurements in polycrystalline samples performed on **1b**, **1c**, and **2′b** indicate high-spin Co^{II} (S = 3/2) in an axially distorted environment. The single-crystal EPR spectroscopic experiment allowed us to determine the ***g***-tensor orientation for a low symmetry Co^{II} compound. Structural and EPR spectroscopic results suggest similar ***g***-tensor orientations for all the compounds and the electronic properties of the Co^{II} ions seem to be independent of the type of halide coordinated to the metal site.

Experimental Section

General Procedures and Materials

All reactions and manipulations of solutions were performed under an argon atmosphere using Schlenk techniques. Solvents were reagent grade and were dried according to literature methods. $CoCl_2$ and CoI_2 were purchased from Aldrich and the α-diimine ligands were synthesized as described elsewhere.[37]

Physical Methods

Infrared spectra were recorded as Nujol mulls on NaCl plates using a Mattson Satellite FTIR spectrometer. Elemental analyses were performed at the Analytical Services of the Laboratory of REQUIMTE. Mass spectra were recorded using an HP298S GC/MS system by the Mass Spectra Service of the Universitat Autònoma de Barcelona, Spain.

X-band CW EPR spectra of polycrystalline samples and single-crystal samples were taken at 4.6 K with a Bruker EMX spectrometer using a rectangular cavity with 100 kHz field modulation, and equipped with an Oxford continuous flow cryostat. The EPR parameters of powdered samples were obtained from spectral simulations using the program Simfonia (v. 1.25, Bruker Instruments Inc.). Powder samples for EPR spectroscopy were obtained by grinding single crystals.

The samples for the single-crystal EPR spectroscopic measurements were oriented by gluing the *cb* and *ca* faces of **1b** and **1c**, respectively, to a cleaved KCl cubic holder, which defines a set of orthogonal laboratory axes. The habit of the crystals was determined by measuring the angles between crystal faces using a goniometric microscope. The sample holder was introduced into a 4 mm OD quartz tube, and positioned in the center of the microwave cavity (see ref.[38] for details). The tubes were attached to a goniometer and the sample was rotated in steps of 10° with the magnetic field in three crystal planes.

Synthesis of Complexes

Synthesis of [Co(*o*,*o*′,*p*-$Me_3C_6H_2$-DAB)Cl_2] (1b): A suspension of $CoCl_2$ (0.26 g, 2 mmol) in CH_2Cl_2 (20 mL) was treated with a yellow solution of *o*,*o*′,*p*-$Me_3C_6H_2$-DAB, (0.64 g, 2 mmol) in CH_2Cl_2 (30 mL), a color change was observed almost immediately from the blue of the initial suspension to green. The mixture was left stirring at room temperature for about 2 h until everything was dissolved. The solution was filtered, and concentrated by vacuum removal of the solvent. A green crystalline solid precipitated, which was separated by filtration, washed with diethyl ether (2 × 10 mL) and petroleum ether (2 × 10 mL), and then recrystallized from hot CH_2Cl_2. **1b** (0.76 g) was obtained in 85% yield.

Compounds **1a** and **1c** were obtained by this method. Yields obtained were between 75 and 85%. Compounds **1a**, **1b**, and **1c** are moisture sensitive.

Synthesis of [Co(*o*,*o*′,*p*-$Me_3C_6H_2$-BIAN)I_2] (2′b): A green suspension of CoI_2 (0.16 g, 0.5 mmol) in CH_2Cl_2 (20 mL) was treated with a red solution of *o*,*o*′,*p*-$Me_3C_6H_2$-BIAN (0.21 g, 0.5 mmol) in CH_2Cl_2 (30 mL). The mixture quickly turned to a red-wine color, and it was stirred overnight until everything was dissolved. After filtration of the solution the solvent was partially removed leaving a dark-red solid, which was separated by filtration, washed with petroleum ether (2 × 10 mL), and then recrystallised from CH_2Cl_2/petroleum ether. **2′b** (0.29 g) was obtained in 78% yield.

Crystallography: Single crystals of complexes **1a**, **1b**, **1c**, and **2′b** were mounted on a Nonius Kappa-CCD area detector diffractometer (Mo-K_α λ = 0.71073 Å). The complete conditions of data collection (DENZO software) and structure refinements are given below. The cell parameters were determined from reflections taken from one set of 10 frames (1.0° steps in phi angle), each at 20 s exposure. The structures were solved by direct methods (SHELXS97) and refined against F^2 using the SHELXL97 software.[27] The absorption was not corrected. All non-hydrogen atoms were refined anisotropically. Hydrogen atoms were generated according to stereochemistry and refined using a riding model in SHELXL97. Some disorders have been fixed for solvent molecules in the case of **1b** and **2′b** complexes (for details, see the corresponding cif files). The fully-labeled ORTEP views have been deposited as supplementary materials. CCDC-297433–297436 contain the supplementary crystallographic data for this paper. These data can be obtained free of charge from The Cambridge Crystallographic Data Centre via www.ccdc.cam.ac.uk/data_request/cif.

1a: Green single crystal, dimension: 0.10 × 0.10 × 0.10 mm. $C_{16}H_{16}Cl_2CoN_2$, M = 366.14 g mol^{-1}; orthorhombic; space group $P2_12_12_1$; a = 10.5880(4) Å; b = 8.2160(3) Å; c = 19.1880(9) Å; Z =

4; $D_{calcd.}$ = 1.457 g cm^{-3}; μ(Mo-K_α) = 1.342 mm^{-1}; a total of 14084 reflections; 2.20° < θ < 30.00°, 4806 independent reflections with 3211 having $I > 2\sigma(I)$; 191 parameters; final results: R_1 = 0.1149; wR_2 = 0.1256, Gof = 1.179, Flack x; 0.00(7), maximum residual electronic density = 0.614 e Å^{-3}.

1b: Green single crystal, dimension: 0.10 × 0.08 × 0.03 mm. $C_{22}H_{28}Cl_2CoN_2$, CH_2CL_2, M = 535.22 g mol^{-1}; monoclinic; space group $P2_1/c$; a = 12.686(5) Å; b = 14.514(5) Å; c = 14.180(5) Å; β = 90.76(5)°; Z = 4; $D_{calcd.}$ = 1.362 g cm^{-3}; μ(Mo-K_α) = 1.079 mm^{-1}; a total of 9800 reflections; 2.13° < θ < 29.98°, 7555 independent reflections with 4498 having $I > 2\sigma(I)$; 268 parameters; final results: R_1 = 0.0733; wR_2 = 0.2063, Gof = 1.037; maximum residual electronic density = 1.177 e Å^{-3}.

1c: Green single crystal, dimension: 0.13 × 0.10 × 0.08 mm. $C_{28}H_{40}Cl_2$ CoN_2, M = 534.45 g mol^{-1}; orthorhombic; space group $Pnma$; a = 10.4110(10) Å; b = 12.707(2) Å; c = 21.311(4) Å; Z = 4; $D_{calcd.}$ = 1.259 g cm^{-3}; μ(Mo-K_α) = 0.816 mm^{-1}; a total of 33608 reflections; 1.91° < θ < 29.83°, 3965 independent reflections with 2385 having $I > 2\sigma(I)$; 154 parameters; final results: R_1 = 0.0614; wR_2 = 0.2027, Gof = 0.825, maximum residual electronic density = 0.324 e Å^{-3}.

2′b: Brown single crystal, dimension: 0.08 × 0.07 × 0.06 mm. $C_{30}H_{28}CoI_2N_2$, 0.2($C_4H_{10}O$), M = 744.10 g mol^{-1}; orthorhombic; space group $Pcca$; a = 16.769(3) Å; b = 11.676(2) Å; c = 18.313(3) Å; Z = 4; $D_{calcd.}$ = 1.378 g cm^{-3}; μ(Mo-K_α) = 2.219 mm^{-1}; a total of 9862 reflections; 1.74° < θ < 30.04°, 5230 independent reflections with 3769 having $I > 2\sigma(I)$; 168 parameters; Final results: R_1 = 0.0710; wR_2 = 0.2249, Gof = 1.049, maximum residual electronic density = 1.424 e Å^{-3}.

Acknowledgments

Work was supported by Fundação para a Ciência e Tecnologia (Project POCI/QUI/55519/2004) in Portugal and SEPCYT:PICT 2003-06-13872, CONICET PIP 02559/2000, and CAI+D-UNL in Argentina. V. R. thanks Fundação para a Ciência e Tecnologia for a Ph.D. grant (SFRH/BD/13777/2003). T. A. and R. W. thank CPU (France) and CRUP (Portugal) for the Portuguese-French Integrated Action-2006, N° F-27/07. A. C. R., M. C. G. P., and C. D. B. thank the Spanish Research Council (CSIC) for providing a free licence to the Cambridge Structural Database.[39] C. D. B. and M. C. G. P. are members of CONICET-Argentina.

[1] R. Crabtree, M. Mingos, *Comprehensive Organometallic Chemistry III: From Fundamentals to Applications*, (COMC-III), Elsevier, **2006**, and its predecessors COMC-II, 1995, and COMC, 1982.
[2] M. Kobayashi, S. Shimizu, *Eur. J. Biochem.* **1999**, *261*, 1–9.
[3] J. J. R. Fraústo da Silva, R. J. P. Williams, *The Biological Chemistry of the Elements. The Inorganic Chemistry of Life*, Clarendon Press, Oxford, **1991**.
[4] R. J. P. Williams, J. J. R. Fraústo da Silva, *The Natural Selection of the Chemical Elements*, Clarendon Press, Oxford, **1996**.
[5] S. J. Lippard, J. M. Berg, *Principles of Bioinorganic Chemistry*, University Science Books, Mill Valley, California, **1994**.
[6] G. van Koten, K. Vrieze, *Adv. Organomet. Chem.* **1982**, *21*, 151–190, and references therein.
[7] B. Rieger, L. Saunders Baugh, S. Kacker, S. Striegler, *Late Transition Metal Polymerization Catalysis*, Wiley-VCH, Weinheim **2003**.
[8] a) S. D. Ittel, L. K. Johnson, M. Brookhart, *Chem. Rev.* **2000**, *100*, 1169–1203; b) G. J. P. Britovsek, V. C. Gibson, D. F. Wass, *Angew. Chem. Int. Ed.* **1999**, *38*, 429–447; c) V. C. Gibson, S. K. Spitzmesser, *Chem. Rev.* **2003**, *103*, 283–315.
[9] a) M. C. Barral, E. Delgado, E. Gutierrez-Puebla, R. Jimenez-Aparicio, A. Monge, C. Delpino, A. Santos, *Inorg. Chim. Acta* **1983**, *74*, 101–107; b) H. Tom Dieck, M. Haarich, *J. Organomet. Chem.* **1985**, *291*, 71–87; c) M. J. Camazón, A. Alvarez-Valdés, J. R. Masaguer, M. C. Navarro-Ranninger, *Trans. Met. Chem.* **1986**, *11*, 334–336; d) Y. Doi, T. Fujita, JP Patent 10298225 (Mitsui Chemicals Inc., Japan) priority date April 25, **1997**; e) T. V. Laine, M. Klinga, A. Maaninen, E. Aitola, M. Leskelä, *Acta Chem. Scand.* **1999**, *53*, 968–973; f) M. Sieger, K. Hübler, T. Scheiring, T. Sixt, S. Zalis, W. Kaim, *Z. Anorg. Allg. Chem.* **2002**, *628*, 2360–2364; g) M. Sieger, M. Wanner, W. Kaim, D. J. Stufkens, T. L. Snoeck, S. Zalis, *Inorg. Chem.* **2003**, *42*, 3340–3346; h) U. El-Ayaan, A. A.-M. Abdel-Aziz, *Eur. J. Med. Chem.* **2005**, *40*, 1214–1221.
[10] a) T. V. Lainen, K. Lappalainen, J. Liimatta, E. Aitola, B. Löfgren, M. Leskelä, *Macromol. Rapid Commun.* **1999**, *20*, 487–491; b) M. Qian, M. Wang, B. Zhou, R. He, *Appl. Catal. A: Gen.* **2001**, *209*, 11–15; c) C. Bianchini, G. Mantovani, A. Meli, F. Migliacci, *Organometallics* **2003**, *22*, 2545–2547.
[11] a) M. Gasperini, F. Ragaini, *Organometallics* **2004**, *23*, 995; b) M. Gasperini, F. Ragaini, E. Gazzola, A. Caselli, P. Macchi, *Dalton Trans.* **2004**, 3376–3382; c) M. Gasperini, F. Ragaini, S. Cenini, *Organometallics* **2002**, *21*, 2950–2957.
[12] a) I. L. Fedushkin, N. M. Khvoinova, A. Y. Baurin, G. K. Fukin, V. K. Cherkasov, M. P. Bubnov, *Inorg. Chem.* **2004**, *43*, 7807–7815; b) I. L. Fedushkin, V. A. Chudakova, A. A. Skatova, N. M. Khvoinova, Y. A. Kurskii, T. A. Glukhova, G. K. Fukin, S. Dechert, M. Hummert, H. Shumann, *Z. Anorg. Allg. Chem.* **2004**, *630*, 501–507.
[13] A. Abragam, B. Bleaney. *Electron Paramagnetic Resonance of Transition Ions*, Clarendon Press, Oxford, **1970**.
[14] J. A. Weil, J. R. Bolton, J. E. Wertz, *Electron Paramagnetic Resonance. Elementary Theory and Practical Applications*, John Wiley & Sons, Inc., New York, **1994**.
[15] J. Zarembowitch, O. Kahn, *Inorg. Chem.* **1984**, *23*, 589–593.
[16] R. Carlin, *Magnetochemistry*, Springer, Berlin, **1986**.
[17] J. H. Pilbrow, *Transition Ion Electron Paramagnetic Resonance*, Clarendon Press, Oxford, **1990**.
[18] A. Goñi, L. M. Lezama, T. Rojo, M. E. Foglio, J. A. Valdivia, G. E. Barberis, *Phys. Rev. B* **1998**, *57*, 246–251.
[19] J. Krzystek, S. A. Zvyagin, A. Ozarowski, A. T. Fiedler, T. C. Brunold, J. Telser, *J. Am. Chem. Soc.* **2004**, *126*, 2148–2155.
[20] A. Bencini, D. Gatteschi, *Inorg. Chem.* **1977**, *16*, 2141–2142.
[21] A. Bencini, C. Benelli, D. Gatteschi, C. Zanchini, *Inorg. Chem.* **1979**, *18*, 2137–2140.
[22] A. Bencini, C. Benelli, D. Gatteschi, C. Zanchini, *Inorg. Chem.* **1979**, *18*, 2526–2528.
[23] L. C. Dickinson, J. C. W. Chien, *J. Am. Chem. Soc.* **1983**, *105*, 6481–6487.
[24] A. C. Rizzi, C. D. Brondino, R. Calvo, R. Baggio, M. T. Garland, E. E. Rapp, *Inorg. Chem.* **2003**, *42*, 4409–4416, and references therein.
[25] E. Dowty, (**1994**). *ATOMS*, Version 6.0, Shape Software, 521 Hidden Valley Road, Kingsport, TN 37663, USA.
[26] A. L. Spek, *J. Appl. Crystallogr.* **2003**, *36*, 7–13.
[27] G. M. Sheldrick, *SHELXL97*, University of Göttingen, Germany, **1997**.
[28] D. Pountney, M. Vasak, *Eur. J. Biochem.* **1992**, *209*, 335–341.
[29] O. Y. Gavel, S. A. Bursakov, J. J. Calvete, G. N. George, J. J. G. Moura, I. Moura, *Biochemistry* **1998**, *37*, 16225–16232.
[30] N. Bonander, T. Väangard, L. C. Tsai, V. Langer, H. Nar, L. Sjölin, *Proteins: Structure, Function and Genetics* **1997**, *27*, 385–394.
[31] C. A. Bates, J. M. Dixon, J. R. Fletcher, K. W. H. Stevens, *J. Phys. C (Proc. Phys Soc.)* **1968**, *1*, 859–871.
[32] K. W. H. Stevens, *J. Phys. C: Solid St. Phys.* **1970**, *3*, 2387–2391.
[33] M. C. G. Passeggi, *Phys. Stat. SolidiB* **1972**, *54*, 681–689.
[34] M. T. Werth, S.-F. Tang, G. Formicka, M. Zeppezauer, M. K. Johnson, *Inorg. Chem.* **1995**, *34*, 218–228.

[35] R. P. van Stapele, H. G. Beljers, P. F. Bongers, H. Zijlstra, *J. Chem. Phys.* **1966**, *44*, 3719–3725.
[36] L. J. Guggenberger, C. T. Prewitt, P. Meakin, S. Trofimenko, J. P. Jesson, *Inorg. Chem.* **1973**, *12*, 508–515.
[37] a) R. van Asselt, C. J. Elsevier, W. J. J. Smets, A. L. Spek, R. Benedix, *Recl. Trav. Chim. Pays-Bas* **1994**, *113*, 88–98; b) H. Tom Dieck, M. Svoboda, T. Grieser, *Z. Naturforsch., Teil B* **1981**, *36*, 823–832; c) M. Svoboda, H. Tom Dieck, *J. Organomet. Chem.* **1980**, *191*, 321–328.
[38] J. M. Schveigkardt, A. C. Rizzi, O. E. Piro, E. E. Castellano, R. Costa de Santana, R. Calvo, C. D. Brondino, *Eur. J. Inorg. Chem.* **2002**, 2913–2919.
[39] a) F. H. Allen, *Acta Crystallogr., Sect. B* **2002**, *58*, 380–388; b) I. J. Bruno, J. C. Cole, P. R. Edington, M. Kessler, C. F. Macrae, P. McCabe, J. Pearson, R. Taylor, *Acta Crystallogr., Sect. B* **2002**, *58*, 389–397.

Received: May 12, 2006
Published Online: October 5, 2006

